# Technical design concept

## of the experimental station

## at the Russian-German beamline at BESSY-II facility

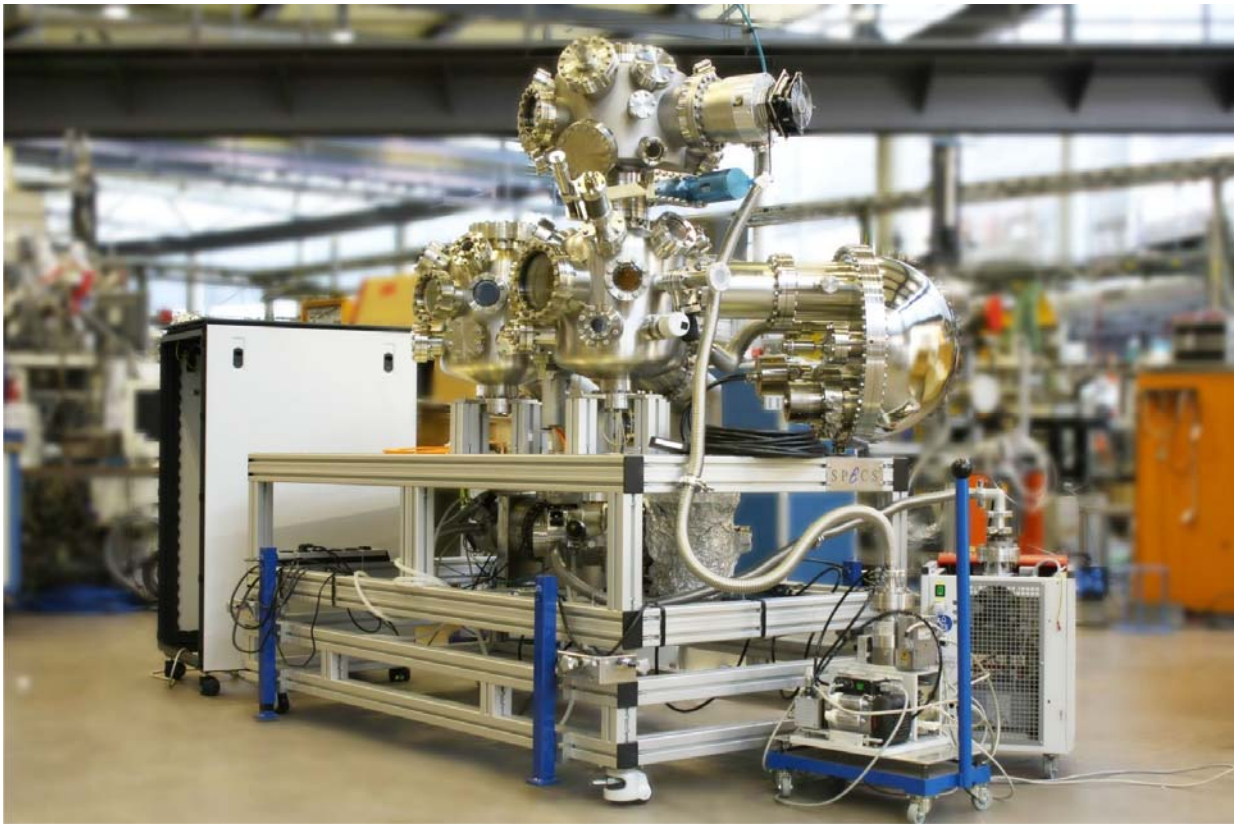

RGL-2011

Designed and assembled by

Dmitry Marchenko (HZB, Berlin)
Oleg Vilkov (TU-Dresden)
Serguei Fedoseenko (Saint-Petersburg University)
Alexander Nelyubov (FU-Berlin)
Andrey Varykhalov (HZB, Berlin)
Denis Vyalikh (TU-Dresden)

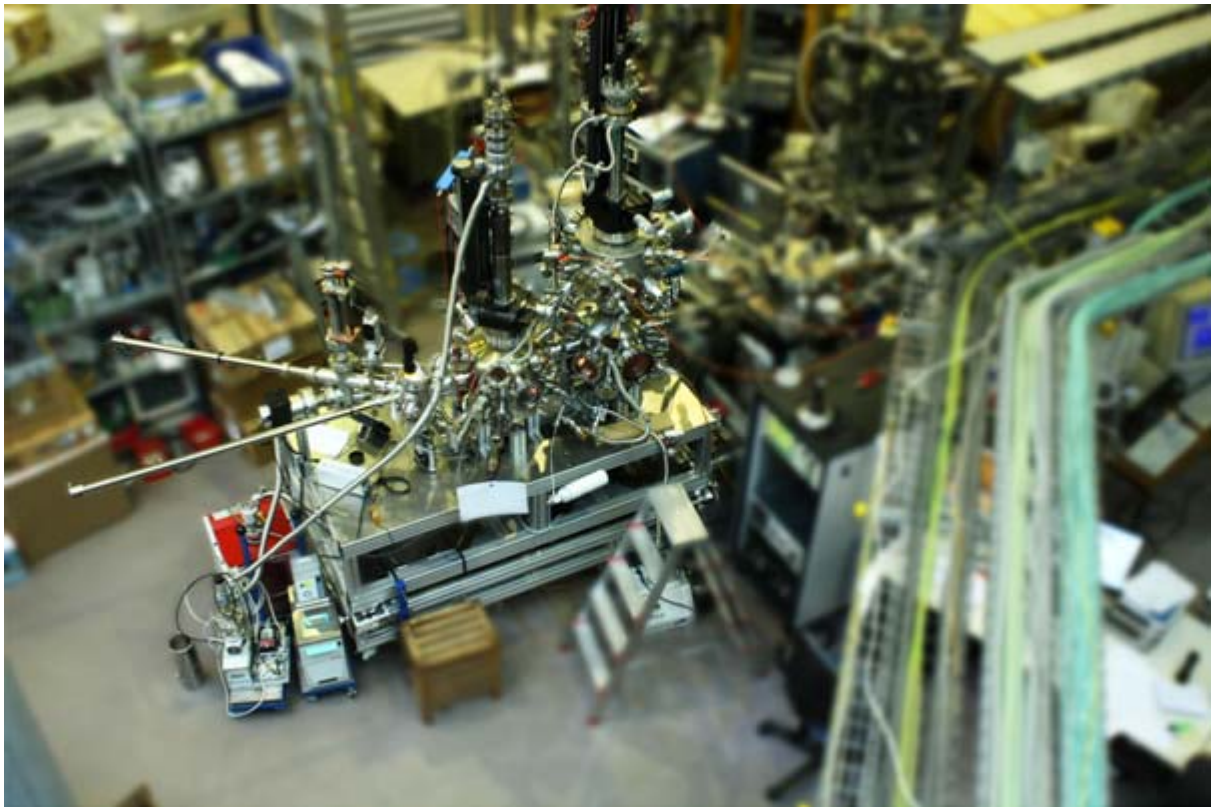

In November 2010 the experimental station at the Russian-German beam line of the BESSY-II facility has been deeply upgraded and is now ready for your experiments. The new instrumentation is very flexible and we expect reliable performance for the whole variety of experiments of our user community. Having several preparation chambers, fast-load systems, a number of insertion devises such as a flash-machine, a cleavage system, a heating stage, a gas-inlet system etc., the station is a powerful instrument allowing to study fundamental properties of matter. Furthermore, an analytical chamber has been configured in a way that it now allows to study a particular physical process or a chemical reaction in real-time.

## General concept

The experimental station is equipped with PHOIBOS 150 electron-energy analyzer with the 2D CCD detector system (SPECS GmbH), which simultaneously offers both energy and angular resolution and allows band mapping as well as high resolution XPS/UPS. The MCP-LEED system (Omicron GmbH) allows to explore

LEED from rather delicate systems like organic molecules and electrically insulating surfaces. The specific advantage of the multi-channel plate (MCP) detector is that it allows electron beam currents down to 0.1 nA. The endstation includes a new cryo manipulator (lowest temperature about 20K) which allows polar and azimuthal rotations of the sample and motions along the x, y, and z axes. It is operated by a set of stepping motors allowing easy handling of the sample with a joystick and quite user-friendly computer interface.

The following brief description shall help our user community to elaborate, prepare and perform sophisticated research programs at the renewed RGL equipment.

### Top preparation chamber

Conceptually, the experimental station consists of three main chambers as it is shown in Figure 1. The “top” preparation chamber is positioned right above the analytical chamber and dedicated for “clean” experiments with rather delicate and reactive materials like rare-earth elements. It is equipped with a quartz microbalance,

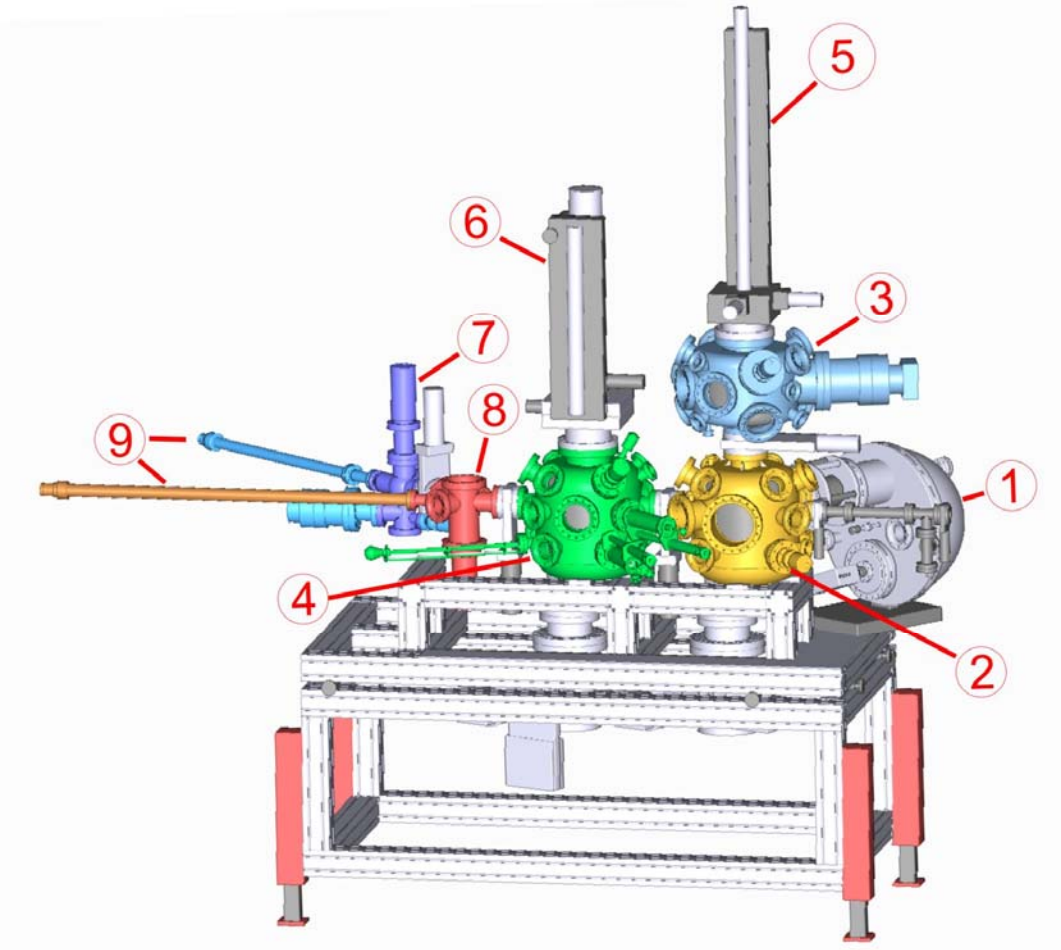


**Figure 1**: 3D overview model of the experimental station. It consists of (1) SPECS PHOIBOS 150 Analyzer, (2) analytical chamber, (3) “top” preparation chamber, (4) “side” preparation chamber, (5) and (6) sample manipulators, (7) and (8) fast-entry system, (9) magnetically coupled sample transporters. It is anticipated that the “top” preparation chamber will be equipped with its own fast-entry system soon.

flanges to mount evaporators (CF35 and CF63), a gas inlet system, a flash-machine, a wobble stick, an ion gun, a few windows, a manipulator and a fast-entry system. Here, thin films can be deposited in-situ from Knudsen cell-type evaporators. Surfaces of bulk samples can be prepared by several methods: (a) cleaving; (b) sputtering; (c) heating up to 2000°C; (d) scraping.

**Analytical chamber: design, available instrumentation and examples of time-dependent experiments**

Measurements are done in the analytical chamber which is equipped with (i) a PHOIBOS 150 electron-energy analyzer, (ii) an MCP-LEED system, (iii) a partial yield electron detector and (iv) an X-ray tube. A port for the installation of a fluorescence detector is foreseen. Optionally, a few flanges CF63/CF35 can be used to mount evaporator sources. This allows time-dependent experiments where metal deposition and PE data acquisition are done simultaneously. It is important to note that only rather non-reactive materials like Ag, Au etc. can be used for this purpose.

Recently, we showed the benefit of disentangling the electronic structure of thin

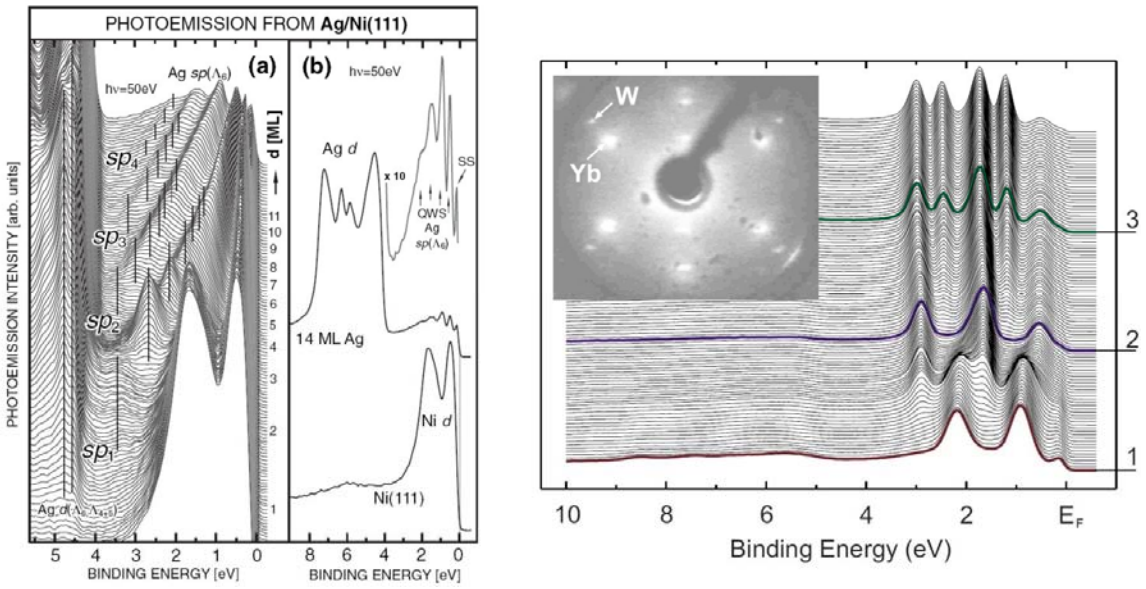


**Figure 2**: *Left panel*: (a) Development of *sp*- and *d*-quantum-well states in Ag overlayers on Ni(111) measured by photoemission upon increasing the thickness of the Ag film up to 14 ML (normal emission). (b) Full range reference photoelectron spectra of clean Ni(111) and of a 14 ML-thick Ag film grown on top. (taken from A. Varykhalov et al., PRL 95, 247601 (2005)). *Right panel:* Experimental angle-resolved PE spectra (5° off-normal) obtained during continuous Yb deposition on W(110) surface. Inset shows LEED image of the 1 ML Yb on W(110). LEED spots of Yb and W lattices are clearly visible indicating different symmetry of the overlayer and the substrate. (taken from Yu. Dedkov et al., PRB 78, 153404 (2008)).

metal films using time-dependent photoemission studies. Figure 2 shows the evolution of photoemission spectra taken from Ag/Ni(111) (left panel) and Yb/W(110) (right panel) during the metal deposition. It allows to pass through all stages of the

formation of thin metallic films beginning from the point when the first atoms of the metal arrive at the surface and subsequently nucleate into the low-dimensional systems.

Another example of time-dependent photoemission is shown in Figure 3. Here it has been applied to study the graphene growth process on a metallic surface during chemical vapor deposition. Most importantly, only by using this approach it was possible to disclose a novel phase of metastable graphene that is characterized by permanent and simultaneous construction and deconstruction. Apparently, this approach allows to provide deep insight into the dynamics of the graphene growth process and to elaborate the experimental conditions for the synthesis of the high-quality graphene flakes.

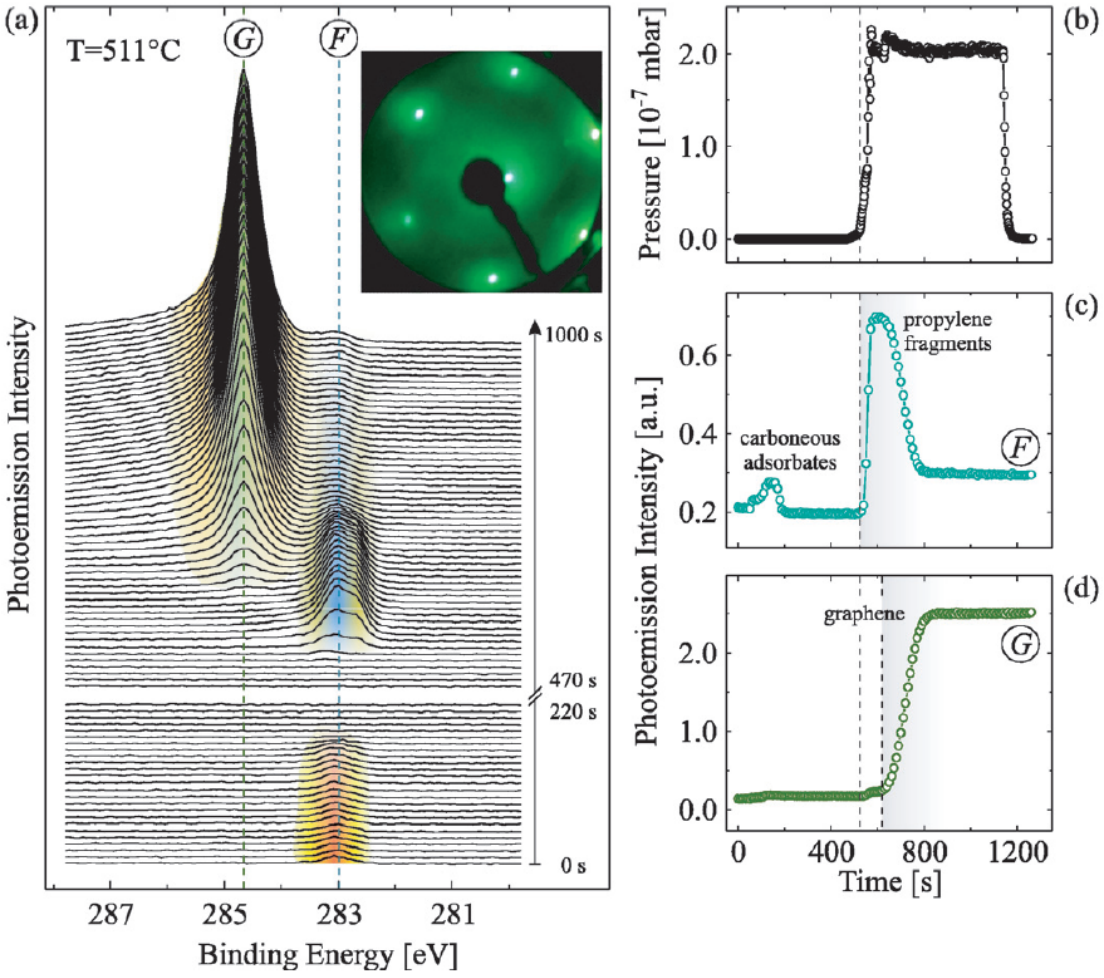


**Figure 3.** (a) Time evolution of the PE intensity in the C 1s region during the graphene growth. Individual scans were taken every ten seconds. F and G mark the signals from $C_3H_6$ fragments and graphene, respectively. The inset shows a LEED pattern (primary energy was 80 eV) after growth of graphene. (b) Partial $C_3H_6$ pressure. (c) and (d) Intensity of the fragment and the graphene C 1s PE signal integrated over ±0.5 eV around their peak maximum. The dashed vertical lines in (b)–(d) indicate the start of the exposure to $C_3H_6$ and the start of graphene growth, respectively. (taken from A. Grüneis et al., NJP 11, 073050 (2009).

The description of the PHOIBOS 150 electron-energy analyzer can be found using the following link:
http://www.specs.de/cms/upload/PDFs/SPECS_Prospekte/phoibos_katalog_72dpi.pdf
The main advantage of the implemented analyzer is the 2D CCD detector system. It simultaneously offers both energy and angular resolution which allows band mapping, angular mapping, and high resolution XPS/UPS measurements. The detector design is especially optimized for the detection of low kinetic energy electrons. Figure 4 shows the band structure taken from Graphene/Ni(111) systems using a similar type of detector. What is to be noted here is that a user-friendly software package has been developed to work with the obtained 2D data sets.

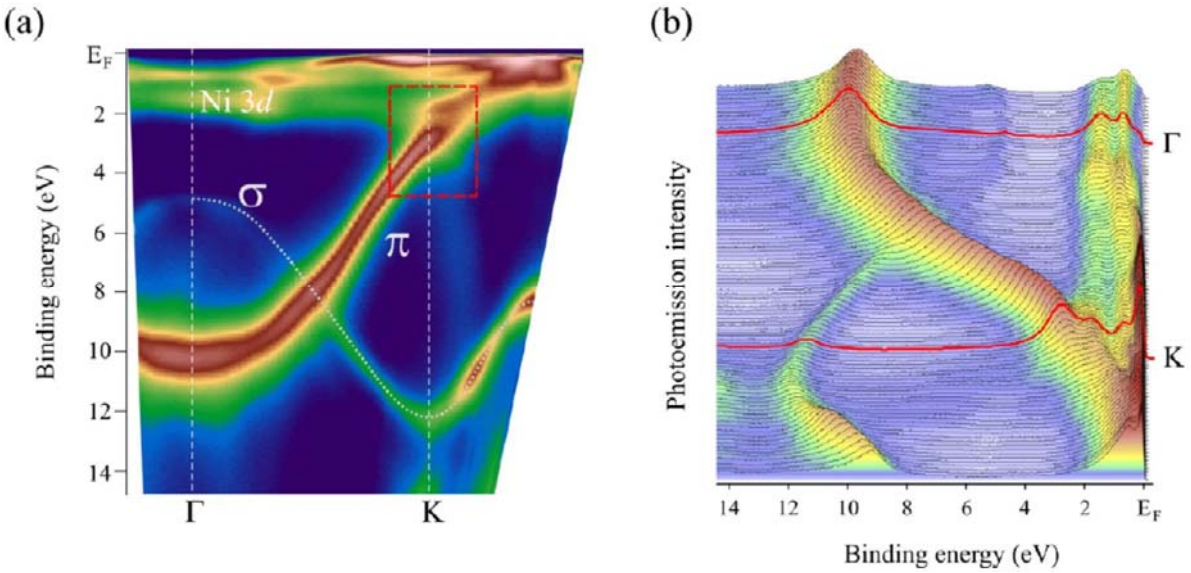


**Figure 4**: Band structure mapping by ARPES of a graphene monolayer synthesized at 550 C. (a) The graphene derived π and σ bands and the Ni 3d bands are depicted. The region around K denoted by a dashed rectangle exhibits the gap in the π band structure, which is due to substrate interaction. (b) The raw ARPES spectra: red lines denote scans taken at Γ and K points, respectively. (taken from A. Grüneis et al., NJP 11, 073050 (2009)).

Additionally, an MCP-LEED system (Omicron GmbH) is installed in the analytical chamber. The main advantage of this instrument is the possibility to explore LEED from rather delicate systems like organic molecules and electrically insulating surfaces. A detailed description of the MCP-LEED instrument can be found here:
http://www.omicron.de/en/products/mcp-leed-/instrument-concept

## Manipulator

The experimental station is equipped with a cryo-manipulator allowing to handle a sample with five degrees of freedom (X, Y, Z, polar and azimuth rotation). Presently, a temperature range of 20-300 K is available. The operation of the cryostat is based on a continuous flow of liquid helium (nitrogen) that is achieved by pulling the liquid gas from the dewar flask through the system, using the diaphragm pump. The design of the sample holder allows to take X-ray absorption spectra at low temperature using the drain-current regime.

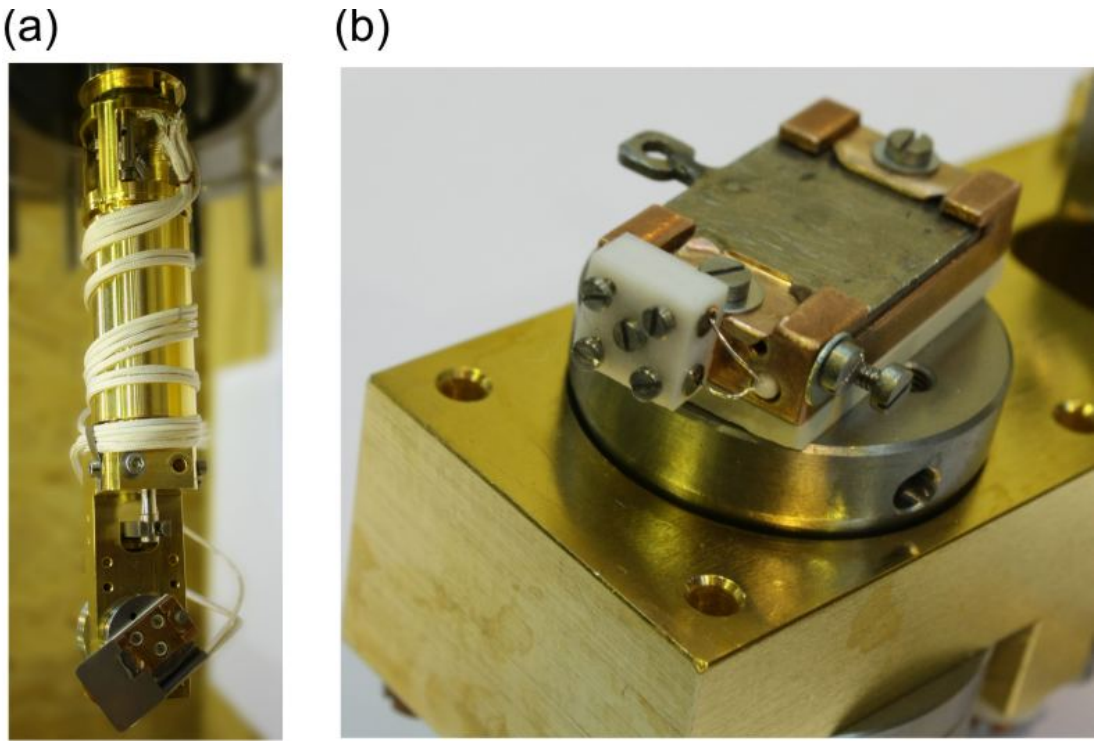


**Figure 5**: Detailed images of the cool-head (a) and sample-holder (b) of the cryo-manipulator.

## Side preparation chamber

The Russian-German dipole beam line was proven to be highly suited for spectroscopic investigations of “fragile” organic and biological molecules which generally show enhanced sensitivity to x-ray damage effects. In order to handle these systems the “side” preparation chamber was elaborated. Basically, it has a similar set of insertion devices as the “top” one, however, it is believed that such delicate materials like organic molecules, polymers, proteins, DNA etc will only be treated in this instrument.

**Transfer system**

The experimental station is equipped with Omicron transfer system, consists of two additional chambers. First chamber (№ 7 on Fig. 1 - “load-lock”) is used for uploading of samples from the air. 11 samples can be uploaded into this chamber simultaneously. This chamber has never direct contact with main chambers (analytical and preparation). The second chamber (№ 8 on Fig. 2) is intermediate between load-lock and side preparation chamber and allows to keep 4 samples. Standard Omicron sample-holders are in use. Maximum width of sample - 10 mm.

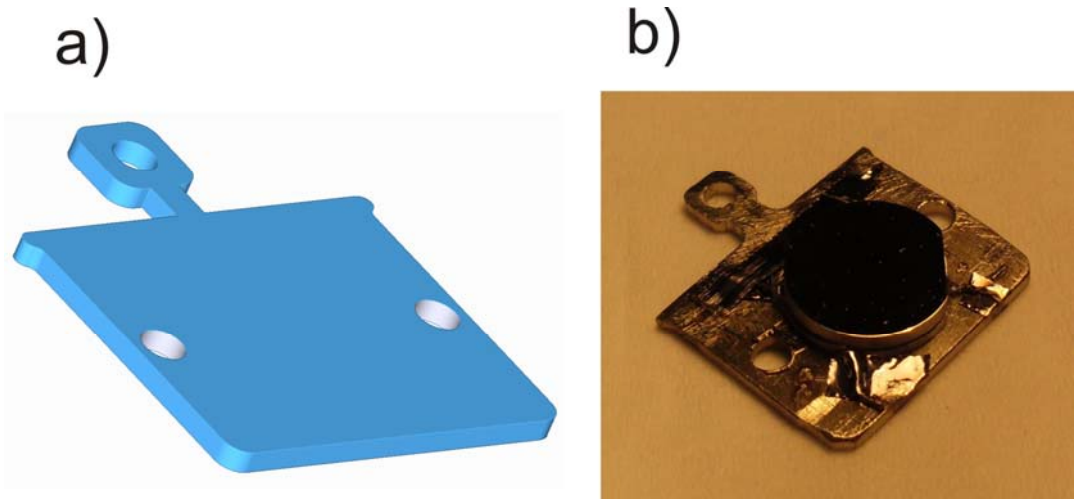


**Figure 6.** General view of sample holder: a - model, b - photo

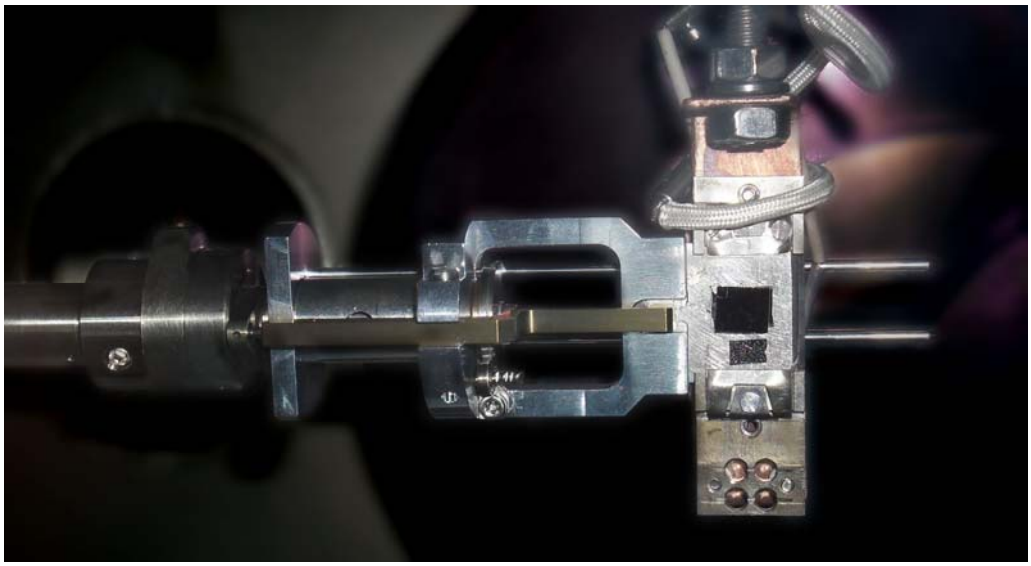

**Figure 7.** Transfer system, sample holder and manipulator in “side” prep. chamber

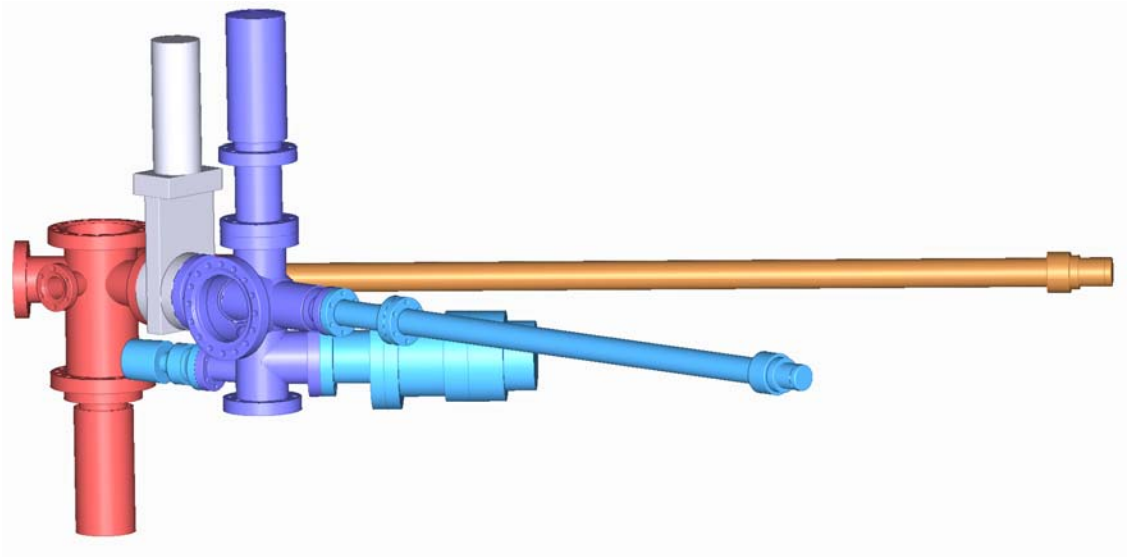

**Figure 8.** Transfer system. View from “load-lock” (model).

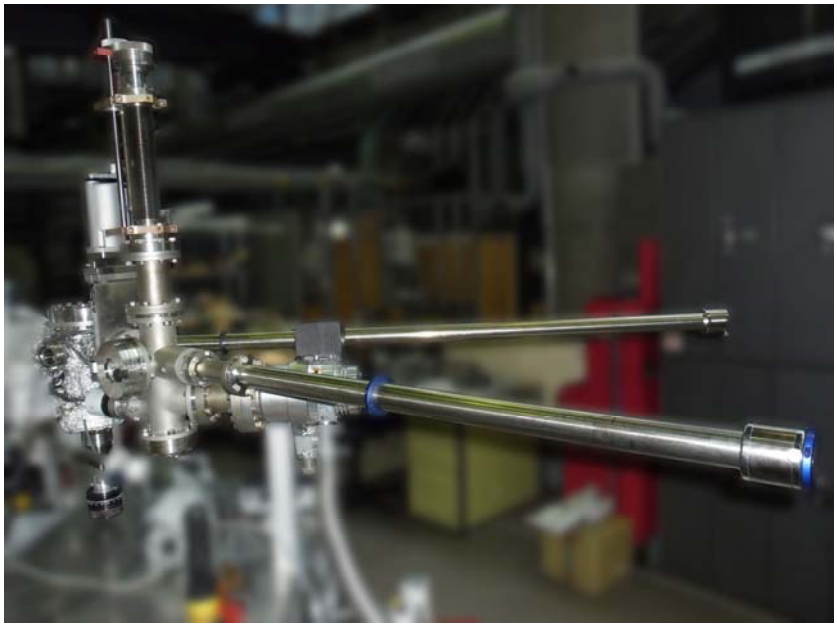

**Figure 9.** Transfer system. View from “load-lock” (photo).

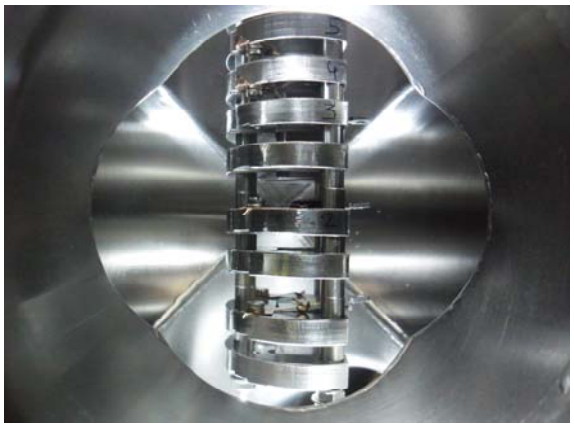

**Figure 10.** Transfer system. “magazine” for 11 samples.

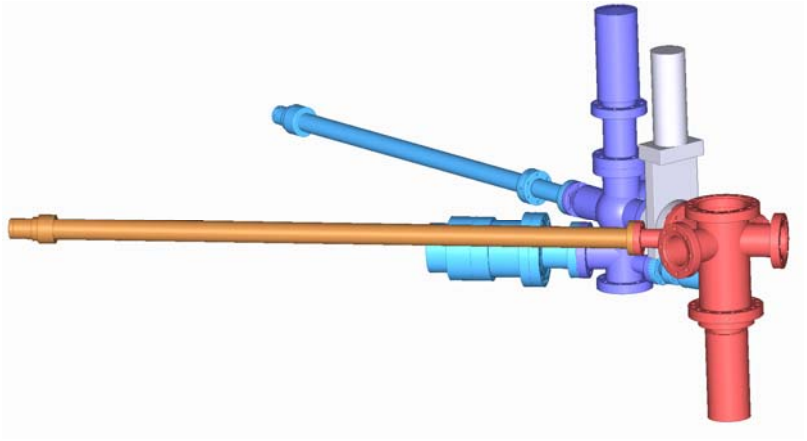

**Figure 11.** Transfer system. View from “second chamber” (model).

**Figure 12.** Transfer system. View from “second chamber” (photo).

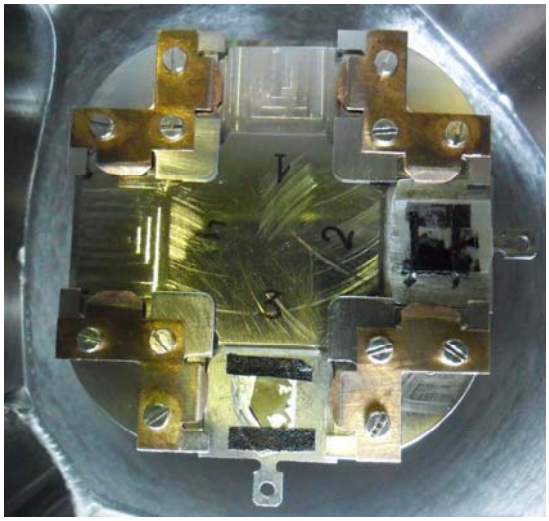

**Figure 13.** “Whirligig” for 4 samples on second transfer chamber.

**Appendix A**

## Design of the analytical chamber

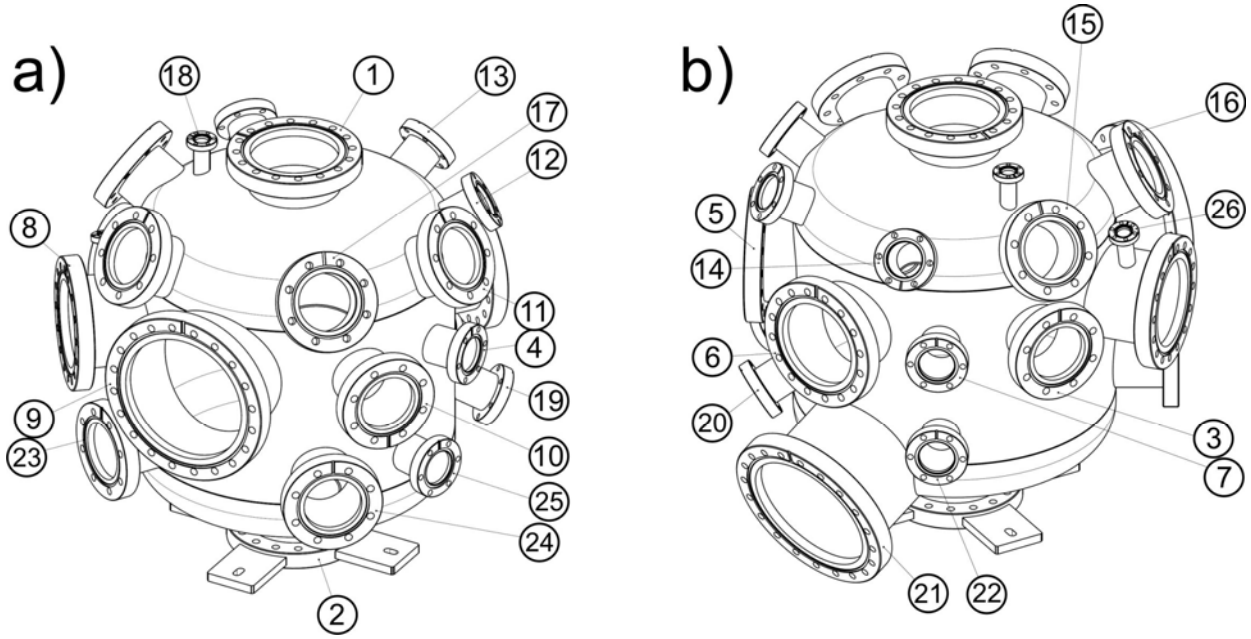


**Figure 14**: Views of the analytical chamber from the (a) beam entrance left side and (b) back side to the beam entrance. The detailed specification of flanges is summarized in the table 1.

Table 1. The specification of flanges located at the analytical chamber.

| No. | Size | Inner Diam. | Port-length | Rot. Angle | Incl. Angle | Inter-section | Bolthole | Bolthole Pos. | Accessory | Remarks |
|---|---|---|---|---|---|---|---|---|---|---|
| *1* | **DN100 CF** | **100.0** | **200.0** | **0.0** | **0.0** | **A** | **clear** | **straddled** | **Vertical preparation chamber** | |
| 2 | DN100 CF | 100.0 | 300.0 | 0.0 | 180.0 | A | clear | straddled | Quartz | |
| **3** | **DN63 CF** | **66.0** | **235.0** | **180.0** | **90.0** | **A** | **clear** | **rotatable** | **Horizontal prepartion Chamber** | |
| **4** | **DN40 CF** | **40.0** | **230.0** | **0.0** | **90.0** | **A** | **clear** | **rotatable** | **Beamline** | |
| **5** | **DN100 CF** | **99.0** | **230.0** | **55.0** | **90.0** | **A** | **clear** | **straddled** | **Analyzer PHOIBOS 150** | |
| 6 | DN100 CF | 100.0 | 240.0 | 110.0 | 90.0 | A | clear | straddled | View port | |
| 7 | DN40 CF | 40.0 | 230.0 | 145.0 | 90.0 | A | clear | straddled | View port | |
| 8 | DN100 CF | 100.0 | 260.0 | 220.0 | 90.0 | A | clear | straddled | View port | |
| 9 | DN160 CF | 150.0 | 254.0 | 270.0 | 90.0 | A | clear | straddled | LEED | optional: View port |
| 10 | DN63 CF | 66.0 | 250.0 | 325.0 | 90.0 | A | clear | straddled | Fluorescent detector | optional: View port |
| 11 | DN63 CF | 40.0 | 250.0 | 0.0 | 60.0 | A | clear | straddled | View port | |
| 12 | DN40 CF | 40.0 | 250.0 | 35.0 | 60.0 | A | clear | straddled | Evaporator | |
| 13 | DN63 CF | 40.0 | 250.0 | 75.0 | 60.0 | A | clear | straddled | Flood gun | |
| 14 | DN40 CF | 40.0 | 250.0 | 135.0 | 60.0 | A | clear | straddled | Leak valve | |
| 15 | DN63 CF | 66.0 | 250.0 | 180.0 | 60.0 | A | clear | straddled | View port | |
| 16 | DN63 CF | 66.0 | 250.0 | 240.0 | 60.0 | A | clear | straddled | View port | |
| 17 | DN63 CF | 66.0 | 250.0 | 310.0 | 60.0 | A | clear | straddled | View port | |
| 18 | DN16 CF | 16.0 | 180.0 | 0.0 | 0.0 | C | clear | straddled | Luminophor | |
| 19 | DN40 CF | 40.0 | 265.0 | 35.0 | 120.0 | A | clear | straddled | Evaporator | |
| 20 | DN40 CF | 40.0 | 270.0 | 75.0 | 120.0 | A | clear | straddled | Evaporator | |
| **21** | **DN160 CF** | **150.0** | **230.0** | **110.0** | **110.0** | **B** | **clear** | **straddled** | **Pump** | |
| 22 | DN40 CF | 66.0 | 230.0 | 145.0 | 90.0 | B | clear | straddled | Vacuum gauge | |
| 23 | DN63 CF | 66.0 | 250.0 | 240.0 | 90.0 | B | clear | straddled | View port | |
| 24 | DN63 CF | 66.0 | 250.0 | 310.0 | 90.0 | B | clear | straddled | View port | |
| 25 | DN40 CF | 40.0 | 230.0 | 345.0 | 90.0 | B | clear | straddled | Vacuum gauge | |
| 26 | DN16 CF | 16.0 | 100.0 | 130.0 | 15.0 | D | clear | straddled | Spare port | |

Flanges, which are marked with bold font, has fixed designation.

Inner diameter of the analytical chamber equals to 360 mm.

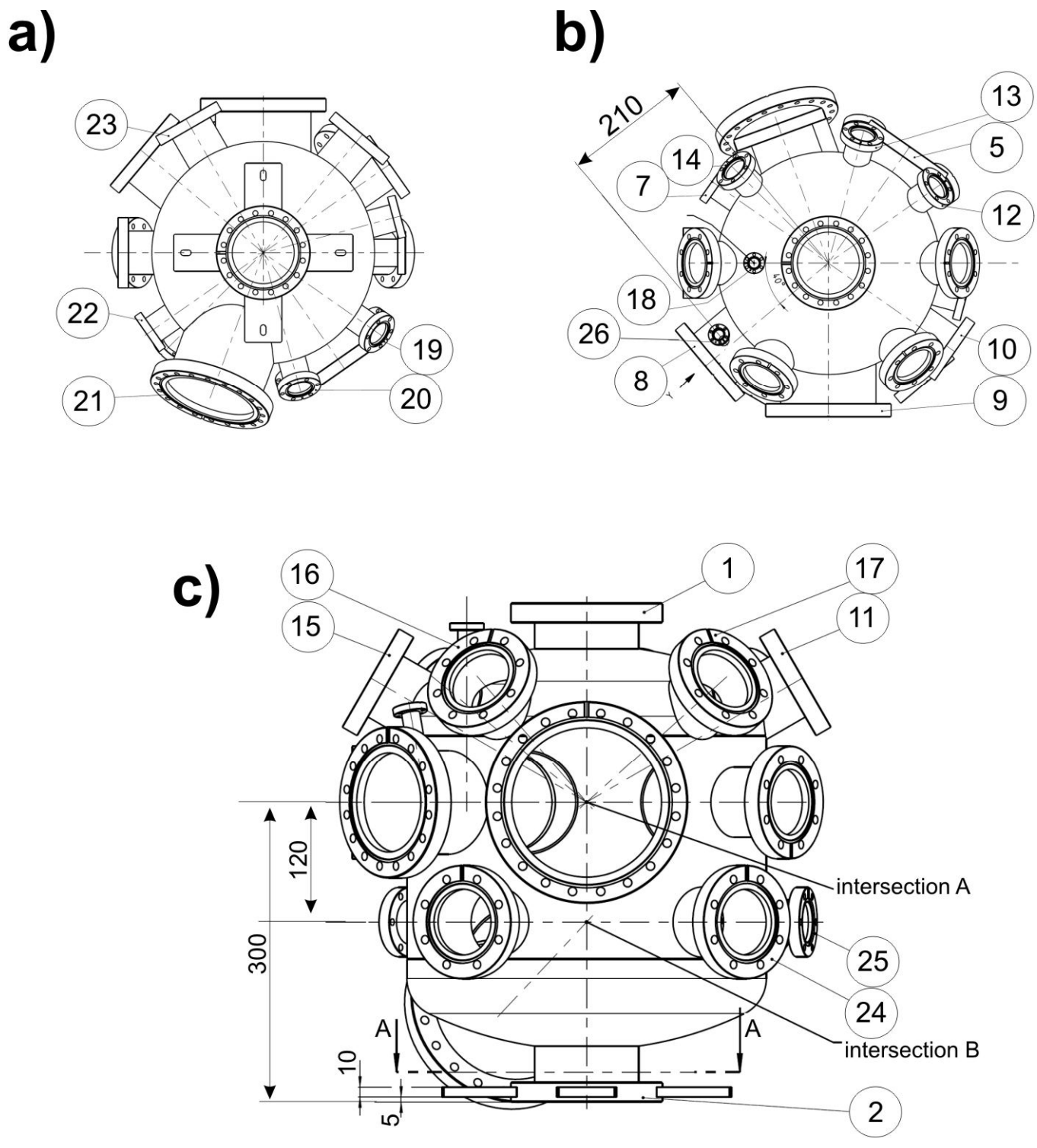


**Figure 15**: Detailed views of the analytical chamber from the (a) bottom, (b) top and (c) beam-entrance left side

**Appendix B**

## Design of the “side” chamber

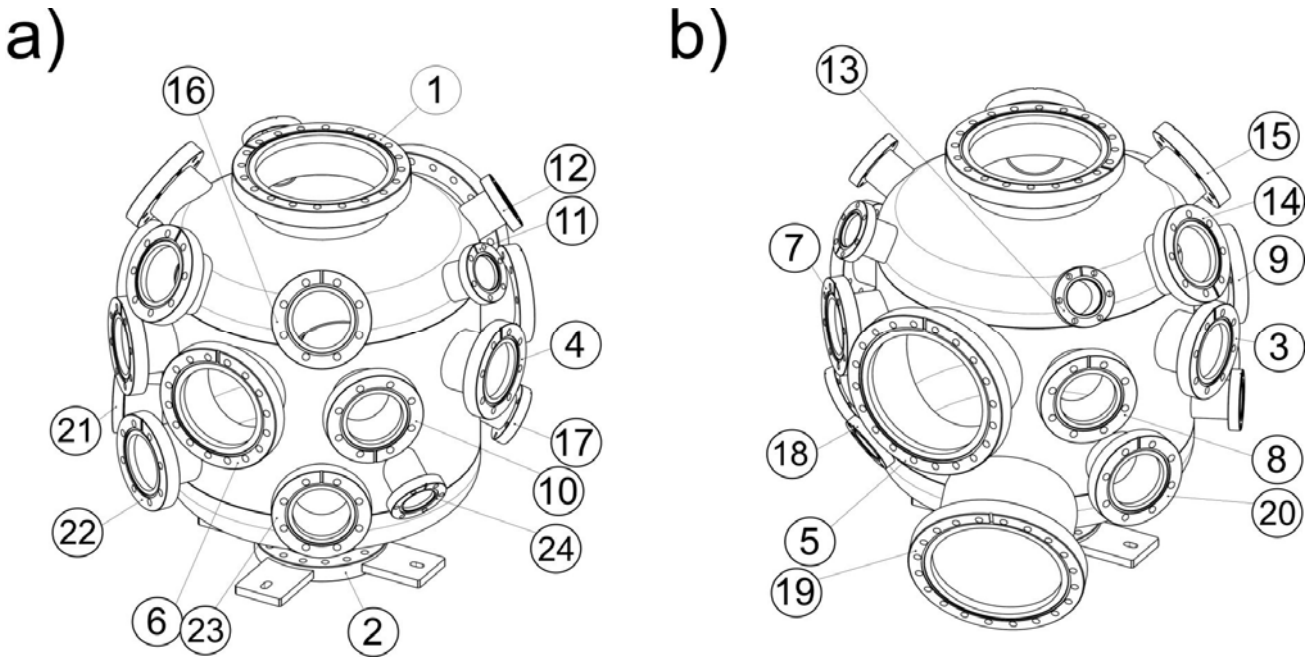


**Figure 16**: Views of the “side” preparation chamber from the analytical chamber entrance (a) left side and (b) back side. The detailed specification of flanges is summarized in the table 2.

Table 2. Supposed using of flanges (“side” preparation chamber)

| | Size | Inner Diam. | Port-length | Rot. Angle | Incl. Angle | Inter-section | Bolthole | Bolthole Pos. | Accessory | Remarks |
|---|---|---|---|---|---|---|---|---|---|---|
| **1** | **DN160 CF** | **150.0** | **200.0** | **0.0** | **0.0** | **A** | **clear** | **straddled** | **Manipulator** | |
| 2 | DN100 CF | 100.0 | 300.0 | 0.0 | 180.0 | A | clear | straddled | Quartz | |
| **3** | **DN63 CF** | **63.0** | **235.0** | **180.0** | **90.0** | **A** | **clear** | **rotatable** | **Transfer** | |
| **4** | **DN63 CF** | **63.0** | **235.0** | **9.0** | **90.0** | **A** | **clear** | **rotatable** | **Analytical Chamber** | |
| **5** | **DN160 CF** | **160.0** | **235.0** | **90.0** | **90.0** | **A** | **clear** | **straddled** | **LEED** | optional: View port |
| 6 | DN160 CF | 160.0 | 250.0 | 270.0 | 90.0 | A | clear | straddled | View port | |
| 7 | DN63 CF | 63.0 | 235.0 | 45.0 | 90.0 | A | clear | straddled | View port | |
| 8 | DN63 CF | 63.0 | 235.0 | 135.0 | 90.0 | A | clear | straddled | View port | |
| 9 | DN63 CF | 63.0 | 235.0 | 225.0 | 90.0 | A | clear | straddled | View port | |
| 10 | DN63 CF | 63.0 | 235.0 | 315.0 | 90.0 | A | clear | straddled | View port | |
| 11 | DN40 CF | 40.0 | 250.0 | 0.0 | 60.0 | A | clear | straddled | Vacuum gauge | |
| 12 | DN40 CF | 40.0 | 250.0 | 45.0 | 60.0 | A | clear | straddled | Mass spectrometer | |
| 13 | DN40 CF | 40.0 | 250.0 | 135.0 | 60.0 | A | clear | straddled | Leak valve | |
| 14 | DN63 CF | 63.0 | 245.0 | 180.0 | 60.0 | A | clear | straddled | View port | |
| 15 | DN63 CF | 63.0 | 245.0 | 240.0 | 60.0 | A | clear | straddled | View port | |
| 16 | DN63 CF | 63.0 | 245.0 | 300.0 | 60.0 | A | clear | straddled | Ion gun | |
| 17 | DN40 CF | 40.0 | 255.0 | 30.0 | 120.0 | A | clear | straddled | Evaporator | |
| 18 | DN40 CF | 40.0 | 255.0 | 60.0 | 120.0 | A | clear | straddled | Evaporator | |
| 19 | DN160 CF | 160.0 | 270.0 | 110.0 | 110.0 | B | clear | straddled | Pump | |
| 20 | DN63 CF | 63.0 | 235.0 | 150.0 | 90.0 | B | clear | straddled | Heater | |
| 21 | DN40 CF | 40.0 | 235.0 | 205.0 | 90.0 | B | clear | straddled | Vacuum gauge | |
| 22 | DN63 CF | 63.0 | 235.0 | 240.0 | 90.0 | B | clear | straddled | Wobble stick | |
| 23 | DN63 CF | 63.0 | 235.0 | 300.0 | 90.0 | B | clear | straddled | View port | |
| 24 | DN40 CF | 40.0 | 255.0 | 330.0 | 120.0 | A | clear | straddled | Evaporator | |

Flanges, which are marked with bold font, has fixed designation.

Inner diameter of the “side” preparation chamber equals to 360 mm.

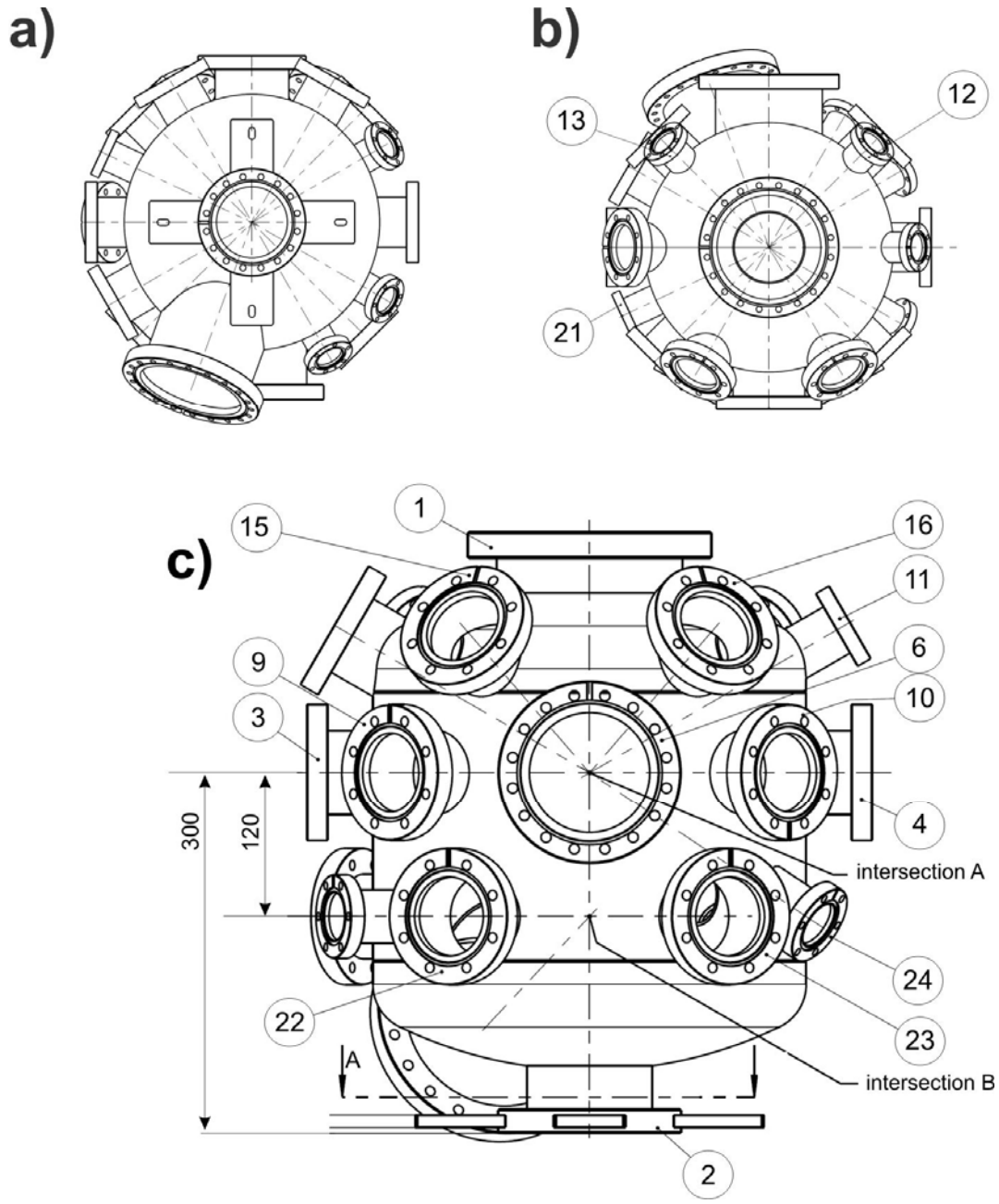


**Figure 17**: Detailed views of the “side” preparation chamber from the (a) bottom, (b) top and (c) left side analytical chamber entrance.

**Appendix C**

## Design of the “top” preparation chamber

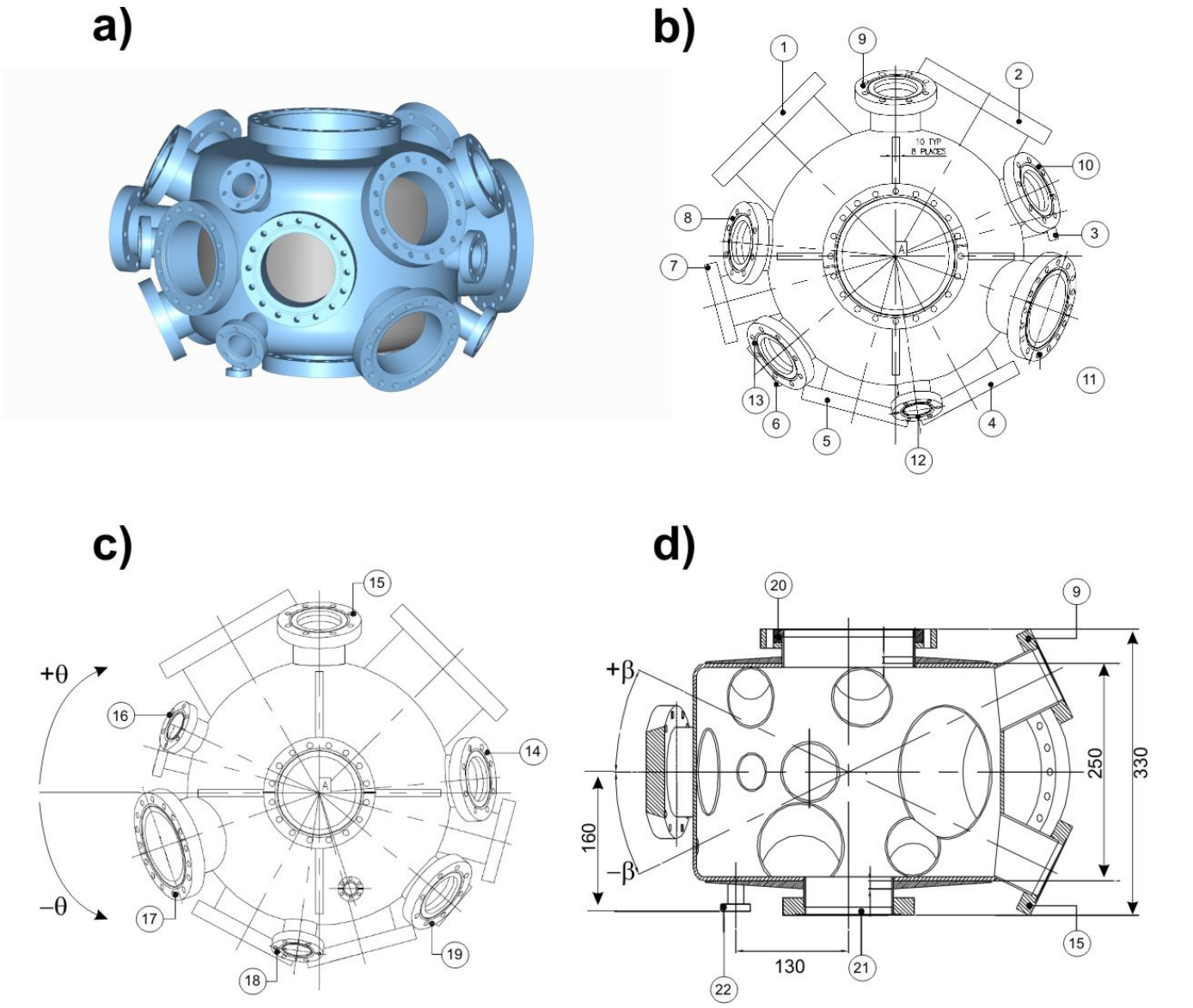


**Figure 18**: Detailed views of the “top” preparation chamber from the (a) bottom, (b) top and (c) left side analytical chamber entrance.

Table 3. Supposed using of flanges (“top” preparation chamber)

| Port № | Flange | Bolthole Pos. | Tube | Focal point | Port length from focal point | Angle β | Angle Θ | Use |
|---|---|---|---|---|---|---|---|---|
| 1* | DN160CF | Rotatable | Tube 152.4x148.3 | A | 260 | 0 | 135 | LEED |
| **2** | **DN160CF** | **Rotatable** | **Tube 152.4x148.3** | **A** | **260** | **0** | **60** | **Pump** |
| 3 | DN40CF | Rotatable | Tube 44.5x4.5 | A | 24 | 0 | 15 | Wobble stick |
| 4 | DN100CF | Straddled | Tube 104x100 | A | 240 | 0 | -82 | Window |
| 5 | DN100CF | Straddled | Tube 104x100 | A | 240 | 0 | -105 | Window |
| 6 | DN40CF | Rotatable | Tube 44.5x40.5 | A | 240 | 0 | -140 | Quartz |
| 7 | DN63CF | Rotatable | Tube 70.0x66.0 | A | 260 | 0 | -165 | Heater |
| 8 | DN63CF | Straddled | Tube 70.0x66.0 | A | 240 | 26 | 175 | Vacuum gauge |
| 9 | DN63CF | Straddled | Tube 70.0x66.0 | A | 260 | 26 | 90 | Window |
| 10 | DN63CF | Straddled | Tube 70.0x66.0 | A | 240 | 26 | 25 | Window |
| 11 | DN100CF | Straddled | Tube 104x100 | A | 250 | 26 | -19 | Window |
| 12 | DN40CF | Straddled | Tube 44.5x40.5 | A | 240 | 26 | -82 | Window |
| 13 | DN63CF | Rotatable | Tube 70.0x66.0 | A | 240 | 26 | -140 | Ion gun |
| 14 | DN63CF | Rotatable | Tube 70.0x66.0 | A | 240 | -26 | 175 | Window |
| 15 | DN63CF | Straddled | Tube 70.0x66.0 | A | 260 | -26 | 90 | Window |
| 16 | DN40CF | Rotatable | Tube 44.5x40.5 | A | 240 | -26 | 25 | Window |
| 17 | DN100CF | Straddled | Tube 104x100 | A | 250 | -26 | -19 | Window |
| 18 | DN40CF | Rotatable | Tube 44.5x4.5 | A | 240 | -26 | -82 | Window |
| 19 | DN63CF | Rotatable | Tube 70.0x66.0 | A | 240 | -26 | -140 | Window |
| **20** | **DN160CF** | **Rotatable** | **Tube 152.4x148.3** | **A** | **165** | **90** | **-** | **Manupulator** |
| **21** | **DN100CF** | **Straddled** | **Tube 104x100** | **A** | **165** | **-90** | **-** | **Analytical chamber** |
| 22 | DN16CF | Rotatable | Tube 19.05x15.8 | - | SEE DRG | -90 | - | Chamber shutter |

* - LEED for flange number 1 is expected.

Flanges, which are marked with bold font, has fixed designation.

Inner diameter of the “top” preparation chamber equals to 360 mm.

**Appendix D.**

**Design of sample holder.**

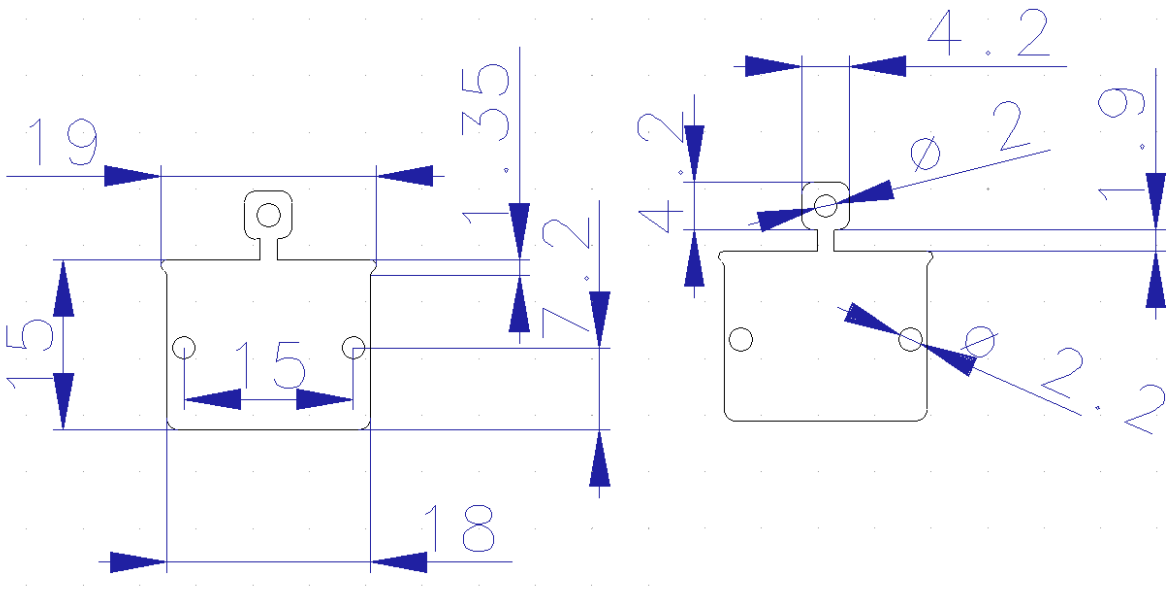


**Figure 19.** Scheme of a sample holder. Width of a sample holder - 1 mm. Left and right side of sample holders should be free (exactly 3 mm from the sides).

**Table of contents.**


General concept 2

Top preparation chamber 3

Analytical chamber: design, available instrumentation and examples of time-dependent experiments 4

Manipulator 7

Side preparation chamber 7

Transfer system 8

Appendix A. Design of the analytical chamber 11

Appendix B. Design of the “side” preparation chamber 14

Appendix C. Design of the “top” preparation chamber 17

Appendix D. Design of sample holder 19

Table of contents 20